



# Development and validation of a routine blood parameters-based model for screening the occurrence of retinal detachment in high myopia in the context of PPPM

Shengjie Li<sup>1,2,3,4</sup> · Meiyang Li<sup>2,3,4,5,6</sup> · Jianing Wu<sup>1</sup> · Yingzhu Li<sup>1</sup> · Jianping Han<sup>1</sup> · Wenjun Cao<sup>1,2,3,4</sup> · Xingtao Zhou<sup>2,3,4,5,6</sup>

Received: 22 December 2022 / Accepted: 14 February 2023 / Published online: 15 March 2023  
© The Author(s), under exclusive licence to European Association for Predictive, Preventive and Personalised Medicine (EPMA) 2023

## Abstract

**Background/aims** Timely detection and treatment of retinal detachment (RD) could effectively save vision and reduce the risk of progressing visual field defects. High myopia (HM) is known to be associated with an increased risk of RD. Evidently, it should be clearly discriminated the individuals with high or low risk of RD in patients with HM. By using multi-parametric analysis, risk assessment, and other techniques, it is crucial to create cutting-edge screening programs that may be utilized to improve population eye health and develop person-specific, cost-effective preventative, and targeted therapeutic measures. Therefore, we propose a novel, routine blood parameters-based prediction model as a screening program to help distinguish who should offer detailed ophthalmic examinations for RD diagnosis, prevent visual field defect progression, and provide personalized, serial monitoring in the context of predictive, preventive, and personalized medicine (PPPM/3 PM).

**Methods** This population-based study included 20,870 subjects (HM = 19,284, HMRD = 1586) who underwent detailed routine blood tests and ophthalmic evaluations. HMRD cases and HM controls were matched using a nested case-control design. Then, the HMRD cases and HM controls were randomly assigned to the discovery cohort, validation cohort 1, and validation cohort 2 maintaining a 6:2:2 ratio, and other subjects were assigned to the HM validation cohort. Receiver operating characteristic curve analysis was performed to select feature indexes. Feature indexes were integrated into seven algorithm models, and an optimal model was selected based on the highest area under the curve (AUC) and accuracy.

**Results** Six feature indexes were selected: lymphocyte, basophil, mean platelet volume, platelet distribution width, neutrophil-to-lymphocyte ratio, and lymphocyte-to-monocyte ratio. Among the algorithm models, the algorithm of conditional probability (ACP) showed the best performance achieving an AUC of 0.79, a diagnostic accuracy of 0.72, a sensitivity of 0.71, and a specificity of 0.74 in the discovery cohort. A good performance of the ACP model was also observed in the validation cohort 1 (AUC = 0.81, accuracy = 0.72, sensitivity = 0.71, specificity = 0.73) and validation cohort 2 (AUC = 0.77, accuracy = 0.71, sensitivity = 0.70, specificity = 0.72). In addition, ACP model calibration was found to be good across three cohorts. In the HM validation cohort, the ACP model achieved a diagnostic accuracy of 0.81 for negative classification.

**Conclusion** We have developed a routine blood parameters-based model with an ACP algorithm that could potentially be applied in the clinic with a PPPM approach for serial monitoring and predicting the occurrence of RD in HM and can facilitate the prevention of HM progression to RD. According to the current study, routine blood measures are essential in patient risk classification, predictive diagnosis, and targeted therapy. Therefore, for high-risk RD persons, novel screening programs and prompt treatment plans are essential to enhance individual outcomes and healthcare offered to the community with HM.

---

Shengjie Li and Meiyang Li contributed equally to this work.

---

✉ Wenjun Cao  
wgkjk@aliyun.com

✉ Xingtao Zhou  
doctzhouxingtao@163.com

Extended author information available on the last page of the article

**Keywords** Retinal detachment · High myopia · Routine blood parameters · Machine-learning · Prediction · Predictive preventive personalized medicine (PPPM/3PM) · Biomarker discovery · Patient stratification

## Introduction

Myopia, exceptionally high myopia (HM), is one of the most common causes of distance vision impairment [1]. Its prevalence is increasing globally [2], especially in Asians [3, 4], making it a public health concern. Approximately half of the world's population will be myopic by 2050, and 10% will be highly myopic [2]. This will increase the visual burden associated with HM. In addition, HM increases the risk of irreversible vision loss from ocular pathologies such as retinal detachment (RD), glaucoma, and myopic macular degeneration [5, 6].

HM is known to be associated with an increased risk of RD [7, 8]. RD is a common cause of visual impairment that impacts about 1% of the world population [8]. Moreover, the incidence of RD has increased from 12.6 per 100,000 people in 2000–2004 to 20.2 in 2015–2019 [9]. The timely detection of RD and treatment by surgery could effectively save vision and reduce the risk of progressing visual field defects [10]. Identifying high-risk individuals is a vital step in preventing RD, according to the European Association for Predictive, Preventive, and Personalized Medicine's (PPPM/3 PM) white paper [11].

Given the rising number of RD patients, it is critical to develop a unique strategy that adheres to the PPPM principles for the early detection of patients with HM who are at a high risk of RD [12]. From the perspective of the PPPM, the early diagnosis of RD and dynamic monitoring by the biomarker/biomarkers panel may open a window of opportunity for targeted prevention and individualized therapy of RD. To achieve this, it is necessary to implement the fundamental tenet of personalized medicine—"one size does not fit all." Hence, a rapid, reliable, and economically feasible clinical model for predicting RD onset in patients with HM is desirable as a screening method rather than relying on professional ophthalmologists and ophthalmic equipment.

It is widely believed that myopia is a multifactorial disease wherein inflammation and environmental factors play a vital role in myopia progression [5, 13, 14]. Some pathogenic mechanisms are associated with RD, but accumulating evidence suggests inflammation plays an essential role in its pathogenesis [15, 16]. Regarding these earlier findings, it is vital to investigate the connection between inflammatory changes and the risk of RD in HM patients, which is in line with the PPPM's guiding principles. It is known that routine blood parameters indicate the general homeostasis and inflammatory state of the whole body. Consequently, from the viewpoints of PPPM in vulnerable populations and individual

monitoring, routine blood parameters could be a novel strategy for the early identification of a high risk of RD in patients with HM [17].

Ophthalmologists would be interested in suggesting a novel strategy for the timely identification of a high risk of RD in patients with HM, in keeping with the PPPM concepts. Machine-learning techniques have been widely used to diagnose eye diseases [18–20]. For example, a PPPM technique for serial monitoring and the development of retrospective data to study the various usage of therapies for macular degeneration and diabetic retinopathy were created by Cheng et al. [21] in an AI-based app using an alternative transformer-based segmentation algorithm. However, there is no clinically validated algorithm for predicting the occurrence of RD in patients with HM. We propose a routine blood parameters-based diagnostic prediction model to decide who should be offered detailed ophthalmic examinations for RD in patients with HM. This study developed a clinically feasible routine blood parameters-based model for the diagnostic prediction of RD, with validation of the model's performance in two cohorts and one HM cohort.

## Working hypothesis

In the context of PPPM [22], a prediction of RD risk classification in the population with HM, more preventative treatment via more accurate screening based on routine blood parameters across visits would be a beneficial and new method for managing patients with HM or RD, as this is presently not extensively implemented in the clinical arena. Thus, a routine blood parameters-based PPPM approach is critical since RD patients would benefit from an objective monitoring approach to prevent visual field defect progression and vision deterioration.

In the framework of PPPM/3 PM, we attempted to design and verify a predictive diagnosis tool for swiftly and correctly triaging patients at high risk of RD. The current study hypothesized that innovative routine blood parameters-based screening programs might be utilized to improve population eye health and develop person-specific, cost-effective preventative and therapeutic measures. To verify the hypothesis and aim of the study, this population-based cross-sectional study included 20,870 individuals who underwent comprehensive routine blood tests and ophthalmic evaluations. We used cost-effective clinical laboratory features to develop and validate a routine blood parameters-based model for the risk classification of RD in the HM population.

## Method

### Study design and setting

This population-based cross-sectional study was done in the Eye and ENT Hospital of Fudan University, Shanghai, China, from June 2015 to June 2022. This study was approved by the Eye and ENT Hospital of Fudan University's Ethics Committee (EENT2015011), which followed the Declaration of Helsinki. In addition, we obtained informed consent from all subjects.

A total of 20,870 unrelated subjects (HM = 19,284, HMRD = 1586) were enrolled in the study after quality control. We used a nested case-control design. First, HMRD cases and HM controls were matched based on age and sex. Then, the HMRD cases and HM controls were randomly assigned to the discovery cohort, validation cohort 1, and validation cohort 2 with a ratio of about 6:2:2. The data split was stratified randomly to ensure that the discovery cohort and the validation cohorts had a similar distribution of data. Other subjects were assigned to the HM validation cohort.

### Inclusion and exclusion criteria

Emmetropia was defined as a mean spherical equivalent (SE) ranging from  $-0.25$  to  $+0.25$  diopters (D). High myopia was defined as a SE of  $\leq -6.00$  D.

Inclusion criteria of HM: (1) age  $\geq 18$  years; (2) SE of  $-6.00$  D or higher. Exclusion criteria of HM: (1) missing refraction data; (2) history of fundus oculi surgery and self-reported refractive surgery; (3) retinal detachment; (4) other types of fundus oculi diseases, such as macular degeneration, diabetic retinopathy, glaucoma and so on; (5) ocular trauma; (6) coagulation disorders; (7) hematologic diseases; (8) received drugs that can affect blood components; (9) systemic diseases, such as infectious diseases, metabolic syndrome, autoimmune disorders, and cancer.

Inclusion criteria of HMRD: (1) age  $\geq 18$  years; (2) SE of  $-6.00$  D or higher; (3) retinal detachment. Exclusion criteria of HMRD: (1) missing refraction data; (2) history of fundus oculi surgery and self-reported refractive surgery; (3) other types of fundus oculi diseases, such as macular degeneration, diabetic retinopathy, glaucoma and so on; (4) ocular trauma; (5) coagulation disorders; (6) hematologic diseases; (7) received drugs that can affect blood components; (8) systemic diseases, including acute infectious diseases, metabolic syndrome, autoimmune disease, and cancer.

All patients underwent a comprehensive ophthalmologic and medical examination. In this study, patients with a missing value (such as age and sex) were excluded.

### Ophthalmic and medical examinations

All patients underwent a comprehensive ophthalmologic examination as described previously [23–25]. As described previously, all subjects were examined by their respective specialty physicians at Fudan University's Eye and ENT Hospital [26–28]. The examinations included slit-lamp examination, uncorrected distance visual acuity, corrected distance visual acuity, autorefractometry, manifest refraction, intraocular pressure (IOP), and funduscopy examinations. Digital retinal camera analysis of their fundi was performed (TRC-NW200, Topcon). The central corneal thickness, axial length, and anterior chamber depth were all measured using an A-scan ultrasonography (A-Scan Pachymeter, Ultrasonic, Exton, PA, USA).

### Collection and analysis of blood sample

During the morning, blood samples were obtained by venipuncture from the antecubital fossae (anterior elbow veins). Blood was drawn from the participants after 8 h of fasting. Laboratory parameters were measured within 0.5 h after blood samples were collected in ethylenediaminetetraacetic acid tubes. Laboratory tests were performed at the Department of Clinical Laboratory of Eye and ENT Hospital of Fudan University [29].

Quantification of common blood indicators, such as platelet count (PLT), thrombocytocrit (PCT), eosinophil count (EOA), monocyte count (MONOA), white blood cell count (WBC), mean corpuscular hemoglobin concentration (MCHC), red blood cell (RBC), mean corpuscular volume (MCV), mean corpuscular hemoglobin (MCH), hematocrit (HCT), hemoglobin (HGB), neutrophil (NEUTA) (Kobe, Japan). Platelet count divided by lymphocyte count is known as the platelet-to-lymphocyte ratio (PLR). The ratio of neutrophils to lymphocytes (NLR) was established as neutrophil count divided by lymphocyte count. Lymphocyte count divided by monocyte count is known as the lymphocyte-to-monocyte ratio (LMR). The systemic immune-inflammation index (SII) was defined as the neutrophil count  $\times$  platelet count/lymphocyte count. Internal controls were also analyzed daily for 10 years, and no significant changes were found in their coefficient of variations (CVs).

### Selection of the feature indexes

Twenty-two routine blood indexes, including eighteen quantitative feature indexes and four transformed indexes, were included. The quantitative feature indexes included PLT, PCT, EOA, MONOA, WBC, MCHC, RBC, MCV, MCH, HCT, HGB, NEUTA, RDWCV, RDWSD, LYMPHA, BASOA, MPV, and PDW. The four transformed indexes included: PLR, NLR, LMR, and SII.

To select a subset of variables for model development, all candidate variables were ranked by the area under the curve (AUC) value. Only variables with high predictability (AUC > 0.6) were included in the final model to achieve better model performance and offset complexity. In addition, logistic analysis was performed to validate the association between selected feature indexes and HMRD. The significant change in the mean of selected feature indexes between the HM and HMRD group were also estimated.

### Model development and selection

The algorithm of conditional probability (ACP) model, logistic regression model, and classification models are applied to predict the event. The accuracy and AUC values are set as the output of the model. The classification models include decision tree, random forest, C5.0, CHAID, and neural networks. All selected feature indexes were arranged and combined and input into the model. Logistic regression model and classification model analyses were performed using IBM SPSS Modeler 18.0.

All selected feature indexes were arranged, combined, and input into the ACP model. In this study, the Bayesian networks model was used. Use Bayes' theorem to calculate the conditional probability of the event given the condition. This is done by multiplying the probability of the event given the condition by the probability of the condition and then dividing by the probability of the event. This is given by  $P(X|pa(X))$ , where  $P$  is the conditional probability,  $a$  represents each index, and  $pa(X)$  represents the parents of index  $X$  (mathematical formula:  $1 - (1 - P) / (1 - P + P * X)$ ). A similar approach has been recently applied to clinical research [30, 31].

### Sample size

To calculate the minimum total sample size, we used an open-source calculator which is based on the methods described by Obuchowski et al. [32] and Li, et al. [33]. The input parameters were specificity = 0.8 (allowable error = 0.05), sensitivity = 0.8 (allowable error = 0.05), and  $\alpha = 0.025$  (2-tailed). Based on this calculation, the minimum sample size required for the new model development was 247 per group. The total sample size in all our cohorts was at least four times higher than this minimum.

### Statistical analysis

We performed descriptive statistical analyses for all variables, and normality was assessed using the Shapiro–Wilk test. The statistical difference between cases and controls was analyzed using multiple tests. For instance, an independent Student's *t*-test was performed for normally

distributed continuous variables, the Kruskal–Wallis test was done for non-normally distributed continuous variables, and the chi-squared test was used for categorical variables when necessary. In addition, one-way ANOVA analysis was used for normally distributed continuous variables among the three groups. Data of continuous variables were expressed as mean  $\pm$  SD. Data of categorical variables were summarized as frequency and percentage.

Receiver operating characteristic (ROC) curve analysis was performed to calculate the AUC value, and the Youden index maximizing sensitivity plus specificity was applied to determine the best cutoff value. AUC stands for the area under the curve and is a measure used to compare the performance of different models/biomarkers. AUC is calculated by plotting the true positive rate against the false positive rate and measuring the AUC value. A model with a higher AUC accurately distinguishes between the two classes. It measures how well a model can distinguish between two classes (in this case, positive and negative outcomes). In this study, the ability to distinguish between RD and HM patients was determined using the AUC of the ROC curve. When the AUC surpasses 0.8, the diagnostic ability is deemed strong. It is regarded as reasonable when the AUC is higher than 0.7 [34].

The models used to achieve prediction are the ACP model, logistic regression model, decision tree, random forest, C5.0, CHAID, and neural networks. The performance of the diagnostic model was evaluated by metrics including accuracy, sensitivity, specificity, positive predictive value (PPV), negative predictive value (NPV), and AUC with 95% confidence intervals (CIs). The Hosmer–Lemeshow goodness of fit test analyzed calibration.

Univariate and multivariate logistic regression models were used to estimate odds ratios (ORs) and 95% confidence intervals (CIs). *P*-values less than 5% were considered statistically significant. All statistical analyses were performed using MedCalc statistical software and SPSS (version 19.0; SPSS Inc., Chicago, IL, USA).

## Results

### Study participants

A total of 20,870 unrelated subjects (HM = 19,284, HMRD = 1586) were enrolled after quality control. HMRD cases and HM controls were matched, resulting in a total of 3451 subjects available for analysis (HM = 1865, HMRD = 1586). These subjects were randomly assigned to the discovery cohort (HM = 1119, HMRD = 950), validation cohort 1 (HM = 373, HMRD = 318), and validation cohort 2 (HM = 373, HMRD = 318) by a ratio of about 6:2:2 (Fig. 1A). Other HM subjects (HM = 17,419) were assigned to the HM validation cohort.

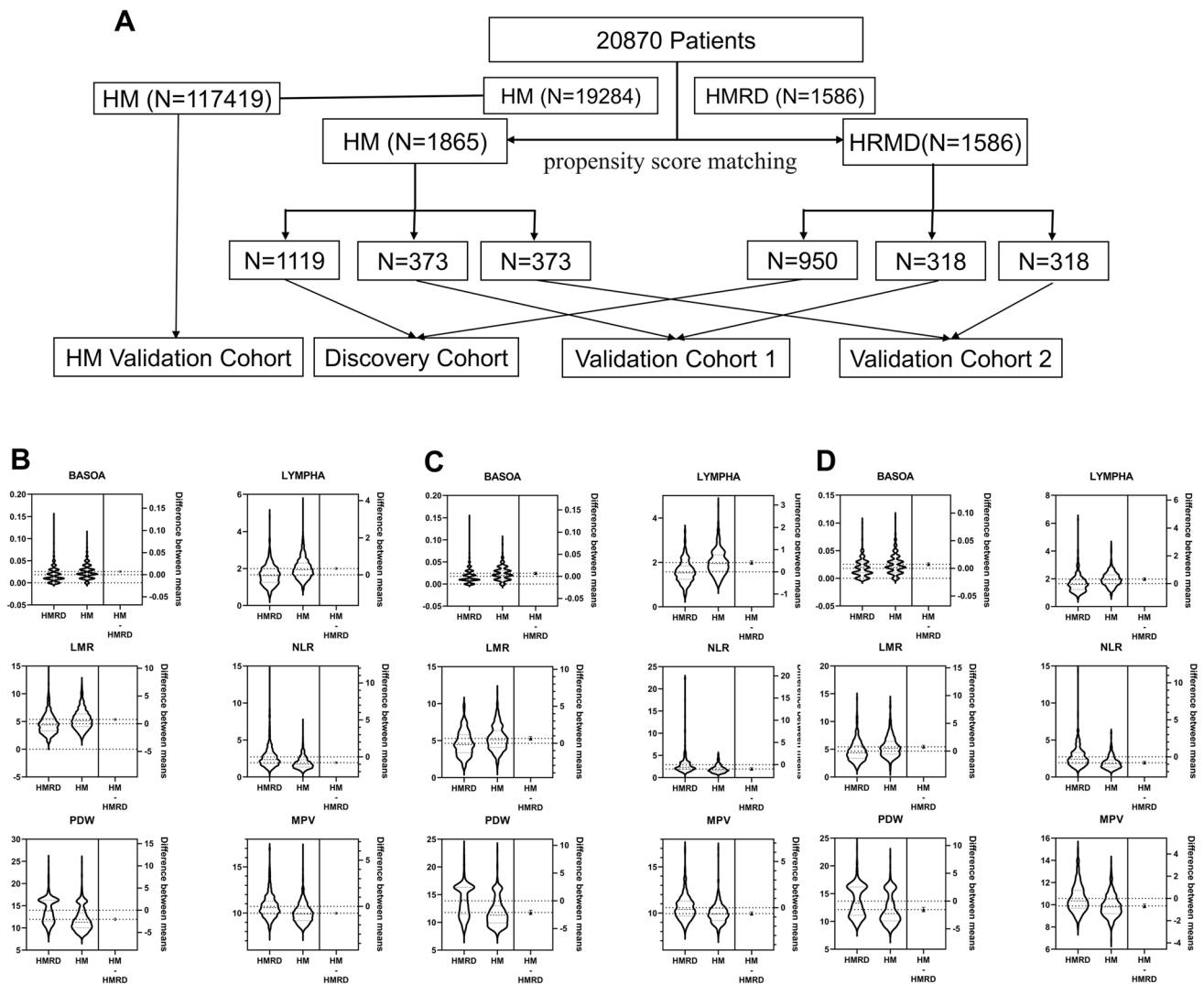


**Fig. 1** Study consort diagram and cohort description. **A** Study consort diagram: flowchart of high myopia (HM) and retinal detachment (RD). **B** Distribution of LYMPHA, BASOA, LMR, MPV, NLR, and PDW between HM and HMRD in the discovery cohort. **C** Distribu-

tion of LYMPHA, BASOA, LMR, MPV, NLR, and PDW between HM and HMRD in validation cohort 1. **D** Distribution of LYMPHA, BASOA, LMR, MPV, NLR, and PDW between HM and HMRD in validation cohort 2

There was no statistical difference in the mean age ( $P > 0.05$ ) and the proportion of sex ( $P > 0.05$ ) between HMRD cases and HM controls among the discovery and validation cohorts and among the discovery cohort, validation cohort 1, and validation cohort 2 (Table 1).

**Feature indexes selection in the discovery cohort**

Figure 2A and Table 2 show the AUC value of the 22 candidate indicators in the discovery cohort. Among the 22 candidate indicators, six candidate indicators (Fig. 2B), namely LYMPHA, BASOA, LMR, MPV, NLR, and PDW, showed better performance ( $AUC > 0.6$ ) in diagnosing RD in patients with HM. The AUC of LYMPHA was 0.68 (95% confidence interval (CI): 0.66–0.70,  $P < 0.001$ ). The AUC

of BASOA was 0.64 (95% CI: 0.61–0.66,  $P < 0.001$ ). The AUC of LMR was 0.63 (95% CI: 0.61–0.66,  $P < 0.001$ ). The AUC of MPV was 0.68 (95% CI: 0.66–0.71,  $P < 0.001$ ). The AUC of NLR was 0.70 (95% CI: 0.67–0.72,  $P < 0.001$ ). The AUC of PDW was 0.72 (95% CI: 0.69–0.74,  $P < 0.001$ ).

**Validation of the feature indexes in the validation cohorts**

In validation cohort 1, six candidate indicators also showed better performance ( $AUC > 0.6$ ) in diagnosing HMRD in patients with HM (Fig. 3A, Table 3). The AUC of LYMPHA was 0.28 (95% CI: 0.24–0.32,  $P < 0.001$ ). The AUC of BASOA was 0.64 (95% CI: 0.60–0.68,  $P < 0.001$ ). The AUC of LMR was 0.61 (95% CI: 0.58–0.65,

**Table 1** Baseline characteristics in the discovery and validation cohorts

Variables	HM	HMRD	<i>P</i> value
Discovery cohort			
Number, <i>n</i>	1119	950	
Age (year)	49.11±8.70	49.32±15.30	0.711
Sex (male)	307 (27.43%)	270 (28.42%)	0.618
Validation cohort 1			
Number, <i>n</i>	373	318	
Age (year)	49.36±9.23	49.34±15.47	0.989
Sex (male)	100 (26.81%)	88 (27.67%)	0.799
Validation cohort 2			
Number, <i>n</i>	373	318	
Age (year)	49.77±9.05	49.29±15.25	0.629
Sex (male)	97 (26.01%)	89 (27.99%)	0.558
<i>P</i> value (age)	0.464	0.999	
<i>P</i> value (sex)	0.860	0.957	

*P* < 0.001). The AUC of MPV was 0.65 (95% CI: 0.61–0.70, *P* < 0.001). The AUC of NLR was 0.71 (95% CI: 0.67–0.75, *P* < 0.001). The AUC of PDW was 0.72 (95% CI: 0.68–0.76, *P* < 0.001).

In validation cohort 2, similar results were observed (Fig. 3B, Table 3). The AUC of LYMPHA was 0.70 (95% CI: 0.66–0.73, *P* < 0.001). The AUC of BASOA was 0.63 (95% CI: 0.59–0.66, *P* < 0.001). The AUC of LMR was 0.64 (95% CI: 0.60–0.67, *P* < 0.001). The AUC of MPV was 0.66 (95% CI: 0.62–0.70, *P* < 0.001). The AUC of NLR was 0.71 (95% CI: 0.67–0.75, *P* < 0.001). The AUC of PDW was 0.67 (95% CI: 0.63–0.71, *P* < 0.001).

**The distributions of feature indexes**

The distributions of LYMPHA, BASOA, LMR, MPV, NLR, and PDW in the discovery cohort (*P* > 0.05), validation cohort 1 (*P* > 0.05), and validation cohort 2 (*P* > 0.05). The distribution of LYMPHA, BASOA, LMR, MPV, NLR, and PDW was similar across the three cohorts, and the distribution of these indicators is shown in Figs. 1 B–D.

**Fig. 2** The area under the receiver operating characteristic (ROC) curves of twenty-two routine blood indexes for prediction of occurrence of retinal detachment in patients with high myopia in the discovery cohort. **A** ROC curve of EOA, HCT, HGB, MCH, MCHC, and MCV. **B** ROC curve of MONOA, NEUTA, PCT, PLR, PLT, and RBC. **C** ROC curve of RDWCV, RDWSD, SII, and WBC. **D** ROC curve of LYMPHA, BASOA, LMR, MPV, NLR, and PDW

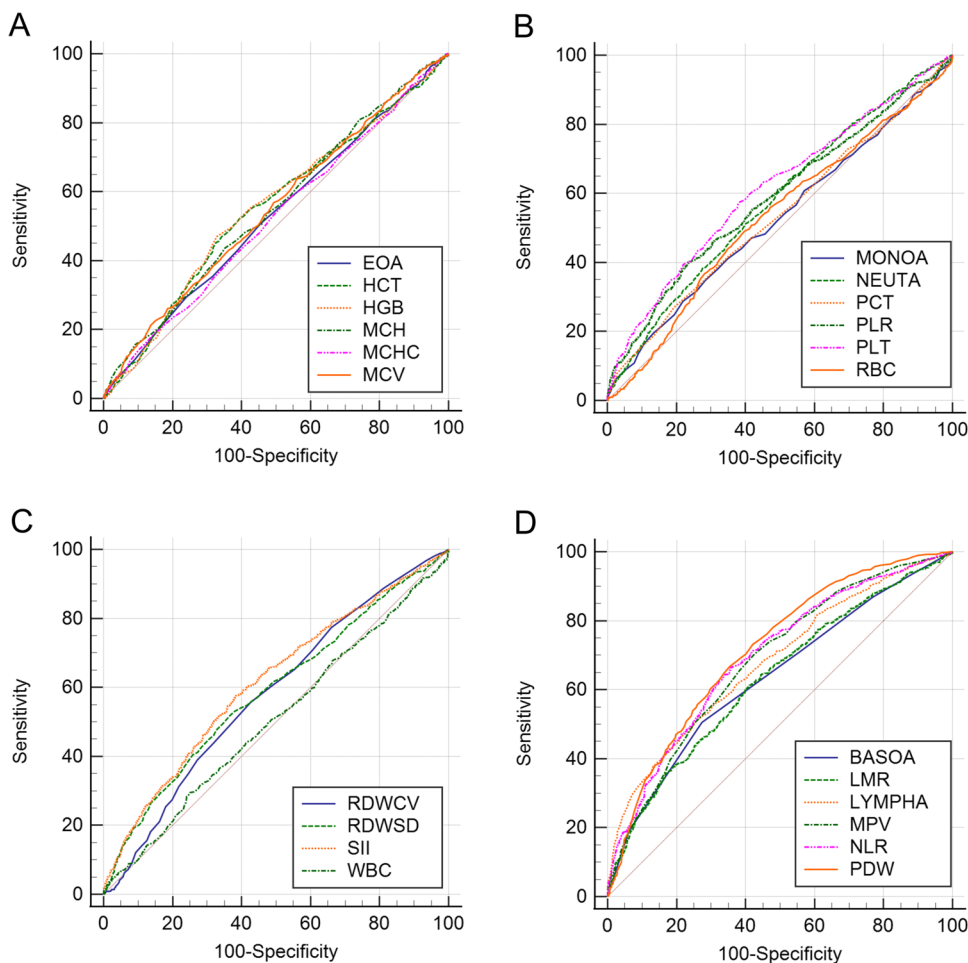


**Table 2** The performance of routine blood index in the discovery cohort

Variable	AUC	S. E	P	95%CI	
				Lower	Upper
AUC (0.5–0.6)					
PLT	0.60	0.01	<0.001	0.58	0.63
PCT	0.53	0.01	0.01	0.51	0.56
EOA	0.53	0.01	0.02	0.51	0.56
MONOA	0.53	0.01	0.04	0.51	0.55
WBC	0.51	0.01	0.69	0.48	0.53
MCHC	0.52	0.01	0.07	0.50	0.55
RBC	0.53	0.01	0.01	0.51	0.56
MCV	0.55	0.01	<0.001	0.53	0.58
MCH	0.55	0.01	<0.001	0.53	0.58
HCT	0.55	0.01	<0.001	0.53	0.58
HGB	0.56	0.01	<0.001	0.53	0.58
NEUTA	0.58	0.01	<0.001	0.55	0.60
RDWCV	0.58	0.01	<0.001	0.55	0.60
PLR	0.59	0.01	<0.001	0.56	0.61
RDWSD	0.59	0.01	<0.001	0.56	0.61
SII	0.60	0.01	<0.001	0.59	0.64
AUC (>0.6)					
LYMPHA	0.68	0.01	<0.001	0.66	0.70
BASOA	0.64	0.01	<0.001	0.61	0.66
LMR	0.63	0.01	<0.001	0.61	0.66
MPV	0.68	0.01	<0.001	0.66	0.71
NLR	0.70	0.01	<0.001	0.67	0.72
PDW	0.72	0.01	<0.001	0.69	0.74

*PLT* platelet count, *PCT* thrombocytocrit, *EOA* eosinophil count, *MONOA* monocyte count, *WBC* white blood cell count, *MCHC* mean corpuscular hemoglobin concentration, *RBC* red blood cell, *MCV* mean corpuscular volume, *MCH* mean corpuscular hemoglobin, *HCT* hematocrit, *HGB* hemoglobin, *NEUTA* neutrophil, *RDWCV* red cell distribution width coefficient of variation, *RDWSD* red cell distribution width standard deviation, *LYMPHA* lymphocyte count, *BASOA* basophil count, *MPV* mean platelet volume, *PDW* platelet distribution width, *PLR* platelet-to-lymphocyte ratio, *NLR* neutrophil-to-lymphocyte ratio, *LMR* lymphocyte-to-monocyte ratio, *SII* systemic inflammation index

Furthermore, the mean levels of BASOA, LYMPHA, and LMR were significantly higher ( $P < 0.001$ ) in HM groups than in HMRD groups in the discovery cohort (Fig. 1B). However, the mean levels of NLR, PDW, and MPV were significantly lower ( $P < 0.001$ ) in HM groups than in HMRD groups in the discovery cohort (Fig. 1B). Similar results were also observed in validation cohort 1 (Fig. 1C) and validation cohort 2 (Fig. 1D).

## The risk of feature indexes for HMRD by logistic analysis

Next, we performed univariate and multivariate logistic regression analyses to validate the relationship between candidate indicators and the risk of HMRD in patients with HM (Table 4). Both univariate and multivariate logistic regression analyses show that a high level of PDW, NLR, and MPV were risk factors for HMRD in patients with HM in the discovery cohort. On the contrary, low levels of LMR, BASOA, and LYMPHA were risk factors for HMRD in patients with HM in the discovery cohort. In validation cohort 1 and validation cohort 2, similar results were observed.

## Diagnostic model development and selection

To further develop the model, we then selected a few candidate variables ranked by AUC value. Finally, the top six better-performing variables, such as LYMPHA, BASOA, LMR, MPV, NLR, and PDW, were chosen for the final model because of their high predictive ability (AUC > 0.6).

Using these six candidate variables, we observed that in the discovery cohort, the ACP model has the highest AUC and accuracy in diagnosing HMRD in patients with HM (AUC = 0.79, accuracy = 0.72). This was followed by the neural networks (AUC = 0.77, accuracy = 0.71), logistic regression (AUC = 0.77, accuracy = 0.70), and other models. The performance of the classification models for HMRD diagnostic is listed in Table 5. These results show that for predicting HMRD in patients with HM, the ACP model is a better performer compared to other models.

Furthermore, 22 features and two demographic factors (age and sex) were integrated into seven algorithm models to compare the performance with the six features-based models. The performance of the 22 features and two demographic factors-based models for HMRD diagnostic is listed in Table S1. The performance between all 24 parameters-based models and six selected features-based models was similar.

## ACP model performance evaluation

The ACP model performance was then evaluated in the discovery cohort, validation cohort 1, and validation cohort 2 (Table 6). The AUC of the ACP diagnostic model was 0.79 (95% CI: 0.77–0.81,  $P < 0.001$ ) in the discovery cohort (Fig. 4A). In the discovery cohort, the ACP model achieved a diagnostic accuracy of 0.72, a sensitivity of 0.71, a specificity of 0.74, a PPV of 0.68, and an NPV of 0.76.

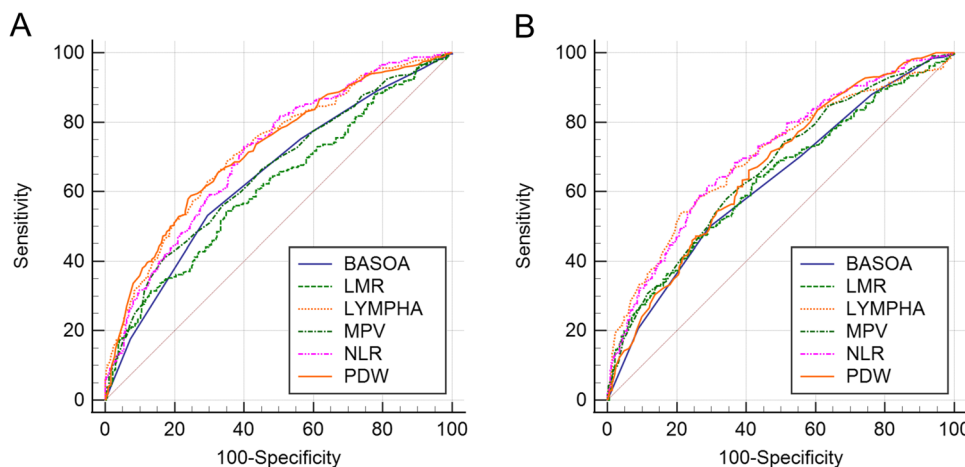


**Fig. 3** The area under the receiver operating characteristic curves (ROC) of LYMPHA, BASOA, LMR, MPV, NLR, and PDW for prediction of occurrence retinal detachment in patients with high myopia. **A** ROC of LYMPHA, BASOA, LMR, MPV, NLR, and PDW

for prediction of occurrence retinal detachment in patients with high myopia in validation cohort 1. **B** ROC of LYMPHA, BASOA, LMR, MPV, NLR, and PDW for prediction of occurrence retinal detachment in patients with high myopia in validation cohort 2

In the validation cohort 1, the ACP diagnostic model achieved an AUC of 0.81 (95% CI: 0.77–0.84,  $P < 0.001$ , Fig. 4B) with a diagnostic accuracy of 0.72, a sensitivity of 0.71, a specificity of 0.73, a PPV of 0.67, and an NPV of 0.77 (Table 6).

In the validation cohort 2, the ACP diagnostic model achieved an AUC of 0.77 (95% CI: 0.73–0.80,  $P < 0.001$ , Fig. 4C) with a diagnostic accuracy of 0.71, a sensitivity of 0.70, a specificity of 0.72, a PPV of 0.64, and an NPV of 0.77 (Table 6).

**Table 3** The performance of selected routine blood index in the validation cohort

Variable	AUC	S. E	$P$	95%CI	
				Lower	Upper
Validation cohort 1					
PDW	0.72	0.02	<0.001	0.68	0.76
NLR	0.71	0.02	<0.001	0.67	0.75
MPV	0.65	0.02	<0.001	0.61	0.70
LMR	0.61	0.02	<0.001	0.58	0.65
BASOA	0.64	0.02	<0.001	0.60	0.68
LYMPHA	0.72	0.02	<0.001	0.68	0.76
Validation cohort 2					
PDW	0.67	0.02	<0.001	0.63	0.71
NLR	0.71	0.02	<0.001	0.67	0.75
MPV	0.66	0.02	<0.001	0.62	0.70
LMR	0.64	0.02	<0.001	0.60	0.67
BASOA	0.63	0.02	<0.001	0.59	0.66
LYMPHA	0.70	0.02	<0.001	0.66	0.73

PDW platelet distribution width, NLR neutrophil-to-lymphocyte ratio, MPV mean platelet volume, LMR lymphocyte-to-monocyte ratio, BASOA basophil count, LYMPHA lymphocyte count

The Hosmer-Lemeshow goodness of fit test showed that the ACP diagnostic model had good calibration in the discovery cohort ( $\chi^2 = 11.363$ ,  $P = 0.182$ ), validation cohort 1 ( $\chi^2 = 9.704$ ,  $P = 0.286$ ), and validation cohort 2 ( $\chi^2 = 4.609$ ,  $P = 0.798$ ) (Table 6).

### ACP model performance evaluation in HM cohort

A total of 17,419 HM patients were assigned to the HM validation cohort. The distributions of HM patients based on the ACP diagnostic model are shown in Fig. 5A. Based on the cutoff value of 0.165, 14,092 subjects ( $> 0.165$ ) were considered HM, and 3327 subjects ( $> 0.165$ ) were considered HMRD (Fig. 5B). In the HM validation cohort, the ACP model achieved a diagnostic accuracy of 0.81 for negative classification.

## Discussion

### Data interpretation

In this study, we considered the PPPM/3 PM strategy for predictive diagnosis RD in patients with HM. We applied the cost-effective clinical routine blood parameters profile to develop and validate the prediction models. As a result, we innovatively developed a routine blood parameters-based ACP model for predictive diagnosis of RD in patients with HM. The ACP model provided marginally better results than the decision tree, random forest, C5.0, CHAID, neural networks, and logistic regression models in terms of AUC and accuracy obtained in the discovery cohort. This is the first study to develop an



**Table 4** Univariable logistic analysis and multivariable logistic analysis in the discovery cohort and validation cohort

	Univariable analysis		Multivariable analysis*	
	OR (95%CI)	P value	OR (95%CI)	P value
Discovery cohort				
PDW	1.189 (1.134–1.246)	<0.001	1.189 (1.134–1.247)	<0.001
NLR	1.654 (1.446–1.892)	<0.001	1.651 (1.443–1.889)	<0.001
MPV	1.321 (1.179–1.481)	<0.001	1.321 (1.178–1.481)	<0.001
LMR	0.936 (0.892–0.923)	0.003	0.937 (0.893–0.923)	0.004
BASOA	0.001 (0.000–0.001)	<0.001	0.001 (0.000–0.001)	<0.001
LYMPHA	0.694 (0.551–0.875)	<0.001	0.689 (0.546–0.869)	0.002
Validation cohort 1				
PDW	1.241 (1.139–1.353)	<0.001	1.236 (1.133–1.348)	<0.001
NLR	1.667 (1.304–2.131)	<0.001	1.671 (1.306–2.136)	<0.001
MPV	1.262 (1.029–1.547)	0.026	1.300 (1.055–1.601)	0.014
LMR	0.785 (0.714–0.862)	<0.001	0.780 (0.709–0.858)	<0.001
BASOA	0.001 (0.000–0.087)	0.019	0.001 (0.000–0.130)	0.023
LYMPHA	0.379 (0.240–0.600)	<0.001	0.358 (0.224–0.570)	<0.001
Validation cohort 2				
PDW	1.217 (1.146–1.293)	<0.001	1.221 (1.149–1.297)	<0.001
NLR	1.903 (1.504–2.407)	<0.001	2.056 (1.702–2.485)	<0.001
MPV	1.560 (1.289–1.888)	<0.001	1.736 (1.476–2.042)	<0.001
LMR	0.873 (0.789–0.965)	0.008	0.873 (0.789–0.965)	0.008
BASOA	0.001 (0.000–0.001)	0.001	0.001 (0.000–0.001)	<0.001
LYMPHA	0.408 (0.287–0.965)	<0.001	0.396 (0.277–0.564)	<0.001

\*Adjusted for gender (male=1, female=2) and age

PDW platelet distribution width, NLR neutrophil-to-lymphocyte ratio, MPV mean platelet volume, LMR lymphocyte-to-monocyte ratio, BASOA basophil count, LYMPHA lymphocyte count

ACP model based on six routine blood parameters to predict RD with high AUC, accuracy, and robustness. This process can improve patient risk stratification and individualized treatment.

In the discovery cohort, the ACP model demonstrated good discrimination between HM patients with and without RD (AUC = 0.79,  $P < 0.001$ , 95% CI = 0.77–0.81). Importantly, model performance was robust in validation cohort 1 (AUC = 0.81,  $P < 0.001$ , 95% CI = 0.77–0.88)

and validation cohort 2 (AUC = 0.77,  $P < 0.001$ , 95% CI = 0.73–0.80). Furthermore, a high diagnostic accuracy (0.81) for negative classification was also achieved in the HM validation cohort. Our results suggest that the routine blood parameters-based ACP model is a good predictor for HMRD and will facilitate the timely identification of high-risk HM subjects to prevent HM progression to RD.

**AI techniques achievements based on fundus image to diagnose RD in the previous studies**

Several investigators have reported fundus image-based models for automated RD detection [35–38]. For example, Lin et al. [37] developed a cascaded deep learning system based on 11,087 ultra-widefield fundus images, which reported a 96.1% sensitivity and a 99.6% specificity with an AUC of 0.989 (95% CI: 0.978–0.996) to detect RD. Meanwhile, Ohsugi and colleagues [36] included 411 ultra-wide-field fundus images and found that the deep learning model demonstrated a high sensitivity of 97.6% (95% CI, 94.2–100%) and a high specificity of 96.5% (95% CI, 90.2–100%), with AUC of 0.988 (95% CI, 0.981–0.995).

**Table 5** Performance of the seven types of models for HMRD prediction

Model	AUC	Accuracy
ACP	0.79	0.72
Random forest	0.75	0.68
C5.0	0.76	0.68
Decision tree	0.75	0.71
CHAID	0.74	0.69
Neural networks	0.77	0.71
Logistic regression	0.77	0.70

**Table 6** The performance of the ACP model\*

	Cutoff	AUC ( <i>P</i> , 95% CI)	Sensitivity	Specificity	PPV	NPV	Accuracy	HL $\chi^2$ ( <i>P</i> value)
Discovery cohort	0.165	0.79 (<0.001, 0.77–0.81)	0.71	0.74	0.68	0.76	0.72	11.363 (0.182)
Validation cohort 1	0.165	0.81 (<0.001, 0.77–0.84)	0.71	0.73	0.67	0.77	0.72	9.704 (0.286)
Validation cohort 2	0.165	0.77 (<0.001, 0.73–0.80)	0.70	0.72	0.64	0.77	0.71	4.609 (0.798)

PPV, positive predictive value; NPV, negative predictive value; HL, Hosmer-Lemeshow test; ACP, algorithm of conditional probability

\*Combined LYMPHA, BASOA, LMR, MPV, NLR, and PDW index

Using dual-stream deep convolutional neural networks, Li et al. displayed consistent performance with high sensitivity, specificity, and AUC on fundus images obtained from clinics to diagnose distinct myopic maculopathy levels (tessellated fundus or pathologic myopia) [38].

Furthermore, a study by Li et al. [39] developed and validation of a deep learning system to screen vision-threatening conditions in HM patients using optical coherence tomography images. The model was trained on a dataset of fundus images from high myopia patients and could accurately detect retinal detachment with an AUC of 0.986.

Fundus image has been an excellent tool for machine learning training in identifying common retinal diseases. Although these fundus image-based models showed better performance, they are unsuitable for screening patients due to their reliance on professional eye examination equipment. Of note, patients rarely visit an ophthalmologist until the symptoms aggravate or visual acuity sharply drops [40]. Therefore, it is hard to predict and diagnose RD early by relying solely on fundus image-based models. Hence, it remains an unmet clinical need to develop a rapid, reliable, and economically feasible screening approach to detect RD.

### Routine blood parameters-based model applied to non-ophthalmic diseases

As we know, there are no other studies with blood-based biomarkers for predicting the occurrence of RD in patients with HM. However, routine blood indexes-based deep-learning algorithms have been successfully applied to non-ophthalmic diseases in recent years [41–45]. For example, using routine blood tests from 15,176 neurological patients, Podnar et al. [42] built a machine learning-based predictive model for the diagnosis of brain tumors and found that the sensitivity of the model was 96% (95% CI, 91–100%), the specificity was 74% (95% CI, 68–79%), and the accuracy was 79% (95% CI, 74–84%). According to data from the UK Biobank cohort, blood-based biomarkers obtained during regular exams are sensitive to both preclinical and clinical cases of colorectal cancer. The final Cox and tree-boosting models achieved a C-index and an AUC of 0.67 and 0.76, respectively [45]. Furthermore, Araújo et al. [46] developed a machine learning-based panel composed of parameters derived from complete blood counts (lymphocytes,

MCV, platelets, and RDW), with an average AUC of 0.91 to predict death by COVID-19. In addition, a recent study suggests that simple blood test abnormalities can be used to identify patients with unexpected weight loss who need further evaluation [47]. Thus, routine blood parameters may contain far more information than recognized, and detecting such non-obvious interrelationships is suitable for developing a machine-learning model for screening diseases.

### Strengths

The routine blood parameters-based ACP model developed in this study is a rapid, reliable, easily accessible, and economical clinical model for the diagnosis of RD. Our study has numerous strengths compared to previously published reports. First, it has only six well-performed indexes, all of which can be completed within 30 min during a routine blood test. Second, the routine blood test is an economic health examination item, costing only 20 Yuan Ren Min Bi (approximately 3 dollars) in China. Third, routine laboratory tests in primary care increase its clinical applicability, avoiding the requirement for professional ophthalmic examination, often only available in a specialized hospital setting. Last, based on the above advantages and good model performance, the routine blood parameters-based ACP model could help decide who should be offered detailed ophthalmic examinations for RD in patients with HM. In addition, the ACP model showed similar predictive performance in the discovery cohort, validation cohorts, and HM validation cohorts. Thus, the routine blood parameters-based ACP could be used in the primary care setting to screen RD in patients with HM.

### Limitations

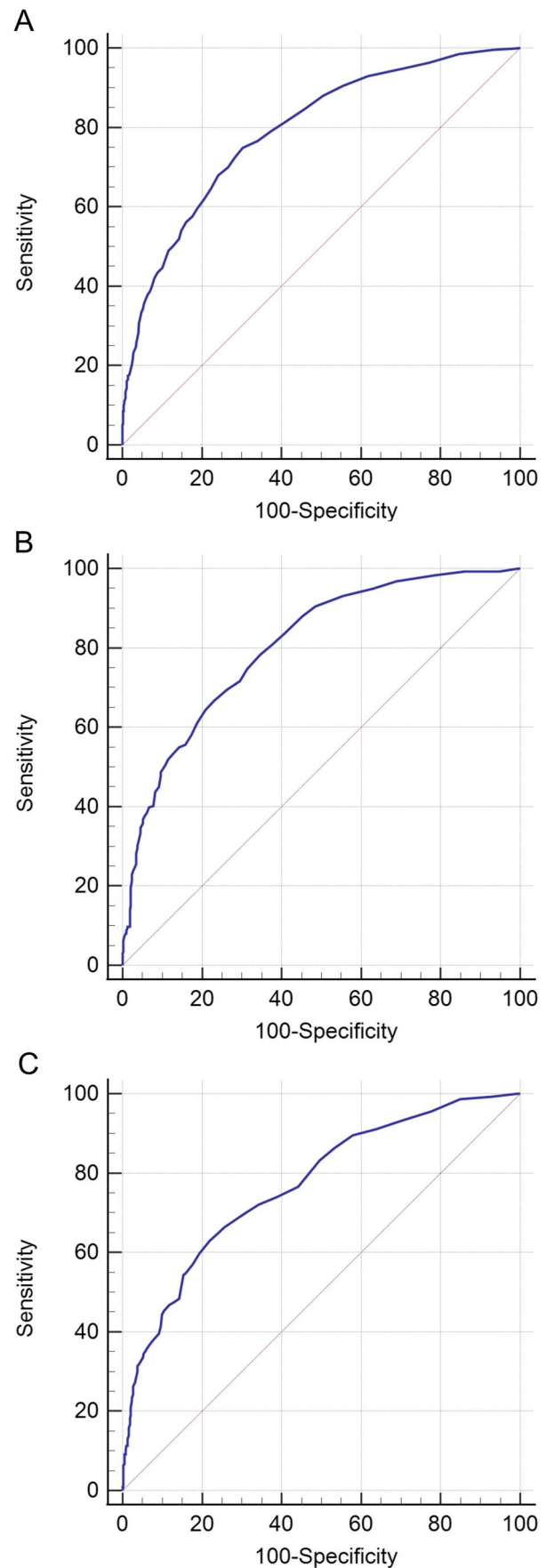
Our study has the following limitations. First, the input data of our ACP model are only routine blood parameters and did not include demographic factors, ophthalmic or other clinical parameters, and other no-routine blood inflammatory factors. Clinical RD evaluation and diagnosis generally require integrated analysis of multiple modalities. Our study only chose routine blood parameters as the input due to their high feasibility and

**Fig. 4** The area under the receiver operating characteristic curves of the ACP model for prediction of the occurrence of retinal detachment in patients with high myopia. **A–C** Predictive performance of the ACP model in the discovery cohort ( $n = 2069$ ), the validation cohort 1 ( $n = 691$ ), and the validation cohort 2 ( $n = 691$ )

widespread availability. Meanwhile, the primary purpose of our study was a proof-of-concept study as to whether routine blood parameters contained sufficient information to predict RD in patients with HM robustly. Future studies are required to further improve the diagnostic performance of the ACP model by incorporating other routine data. Second, the routine blood test was performed using a Sysmex series automated blood counting system (Kobe, Japan). Variability in the results obtained from other automated blood counting systems may limit the application of the ACP model. Third, all the data used for building the ACP model were from patients of one population cohort. However, the population-level changes in the reference level of routine blood indexes should be accounted for across different populations. Hence, this ACP model must be further validated in other populations to determine its broader applicability.

## Conclusions and expert recommendations

Due to the reactive medical approach to disease management, RD reached an epidemic scale worldwide, impacting about 1% of the world population. Moreover, the incidence of RD trends to increase, particularly for individuals with HM. The corresponding socio-economic burden is enormous. Further, clinically manifested RD is only the “tip of the iceberg”: apparently, the total size is about greater in the population than the currently applied reactive medical approach. To this end, we used cost-effective clinical laboratory features to develop and validate a routine blood parameters-based model for the risk. It is a candidate prediction model in predicting patient risk classification, which can be applied for predictive diagnosis of RD in a population with HM. of RD in the HM population. In this work, we have developed an ACP model to predict the onset of RD among HM subjects based on six routine blood parameters, namely LYMPHA, BASOA, LMR, MPV, NLR, and PDW. We established and compared seven models to pre-screen RD in patients with HM, showing that the ACP-based model has the highest overall predictive power. This model may help predict RD in patients with HM, and informed decisions on who should be offered detailed ophthalmic examinations could be made. Furthermore, the model promotes the precise prevention and personalized administration of HM subjects at high risk of RD onset. Accordingly, this supports the paradigm shift from reactive medicine to PPPM/3 PM.



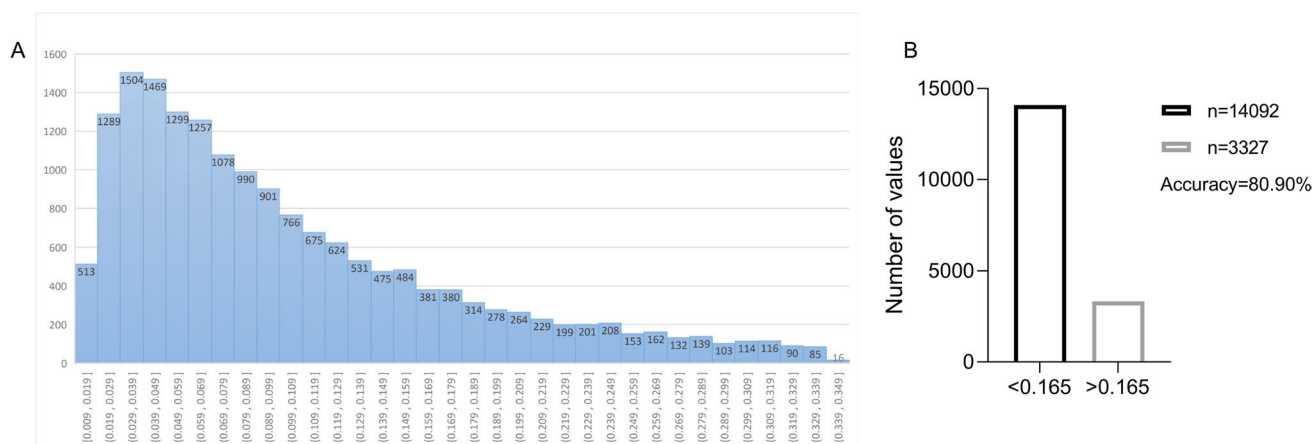


**Fig. 5** The number of high myopia subjects according to the level of ACP model-based value (A). The number of high myopia subjects in the ACP model-based value <0.165 group and >0.165 group (B)

### For the further application routine blood parameters-based model in the context of PPPM in RD management, we recommend the following

**Predictive medical approach** Routine blood indexes-based models have been successfully applied to non-ophthalmic diseases in recent years [41, 42]. The routine blood parameters-based model for ophthalmic diseases yields a better-discriminating power or predictive accuracies for predicting HM individuals likely to develop early-onset RD. It is a candidate prediction model in predicting patient risk classification which can be applied for the predictive diagnosis of RD in population with HM.

**Targeted prevention** The timely detection of RD could prevent visual field defect progression. The early identification of HM individuals with a high risk of RD is a cost-effective way for the targeted prevention of RD diseases. Based on each patient's unique risk profile, this model may enable tailored follow-up and care to lower the risk of advancing visual field abnormalities.

**Personalized treatments** The early diagnosis of RD and timely treatment could effectively save vision. Accumulating evidence suggests inflammation plays an essential role in RD pathogenesis [15, 16]. It is well-recognized that routine blood parameters reflect the body's overall homeostasis and inflammatory status. A high inflammatory state is related to an increased risk of RD. It should be used to justify additional investigation and individualized therapies incorporating anti-inflammatory medicines, nutritional substitutes, and therapy supplements, such as diet and exercise regimens. Consequently, from the viewpoints of PPPM in vulnerable populations and individual monitoring, dynamically monitoring routine blood parameters might be a unique approach that could enhance customized management in the treatment of RD or HM.

### Importantly, what is exactly the added value of our study?

The research described in this study advances our knowledge and will be helpful when evaluating PPPM in RD patients.

First, a model based on routine blood parameters can be a valuable tool for predicting an individual's transition from HM to RD.

Second, to avoid disease progression from HM to RD based on each patient's unique risk profile, a routine blood parameters-based model may provide tailored follow-up and care for each patient.

Finally, routine blood parameters-based models may also be utilized in the future, either alone or in combination with additional biochemical markers, in algorithms to choose the most appropriate course of treatment for each patient, including anti-inflammatory drugs, nutritional supplements, or therapy supplements. For example, (1) several studies reported that anti-inflammatory treatment in RD results in restoration of the anatomical position of the ciliary body and improves reattachment rates [48–50]; (2) according to surveys on lutein and zeaxanthin supplementation, moderate intakes of these nutrients are linked to a lower incidence of RD and reduced visual impairment [51]; (3) Alejandra Daruich et al. [52] performed a clinical trial and reported that oral ursodeoxycholic acid is a potential neuroprotective adjuvant therapy in RD.

### The paradigm shifts from reactive to PPPM/3PM and go beyond the state of the art

- (1) Developing innovative solutions for better predictive, preventative, and customized capability, as well as improved cost-efficiency of healthcare systems based

on a routine blood parameters-based model for screening the incidence of RD in HM in the context of PPPM.

- (2) Risk stratification of RD patients and improvement of individual clinical outcomes at the secondary care level.
- (3) Instead of depending on qualified ophthalmologists and ophthalmic equipment, a simple, accurate, and financially viable clinical model based on routine blood parameters is preferred for predicting the onset of RD in patients with HM.

A crucial part of the PPPM approach during the EPMA World Congress 2019 was the tailored and real-time monitoring of patient biological parameters to enhance therapeutic results [53]. Improving the levels of routine blood parameters might potentially increase both—the quality of vision and the life quality.

Despite routine blood parameters-based model simplicity and quick administration, this predictive tool still needs further validation and calibration in longitudinal studies. Additional prospective data collection in actual primary care settings is required to verify this recent result's validity and further improve the final risk prediction model.

**Supplementary Information** The online version contains supplementary material available at <https://doi.org/10.1007/s13167-023-00319-3>.

**Acknowledgements** The authors would like to thank Sysmex Corporation (Shanghai) for their assistance in statistical analysis.

**Code availability** All software applications used are included in this article.

**Author contribution** SJ. Li: data curation, formal analysis, investigation, visualization, writing—original draft, project administration, writing—review and editing. MY Li: data curation, investigation, visualization, writing—review and editing. JN Wu: data curation, visualization, writing—original draft, project administration, writing—review and editing. YZ Li: resources, investigation, writing—original draft, writing—review and editing. JP Han: resources, investigation, writing—original draft, writing—review and editing. WJ Cao: resources, supervision, funding acquisition, investigation, writing—original draft, writing—review and editing. XT Zhou: resources, supervision, funding acquisition, investigation, writing—original draft, writing—review and editing.

**Funding** This work was supported by Youth Medical Talents – Clinical Laboratory Practitioner Program (2022-65), Shanghai Municipal Commission of Health and Family Planning (20224Y0317), Clinical Research Plan of SHDC (SHDC2020CR1043B), Project of Shanghai Xuhui District Science and Technology (2020-015). The sponsor or funding organization had no role in the design or conduct of this research.

**Data availability** The datasets generated during and/or analyzed during the current study are available from the corresponding author on reasonable request.

## Declarations

**Ethics approval** This study was approved by the Eye and ENT Hospital of Fudan University's Ethics Committee (EENT2015011), which followed the Declaration of Helsinki.

**Consent to participate** Informed consent was obtained from all participants.

**Consent for publication** Not applicable.

**Competing interests** The authors declare no competing interests.

## References

1. Bourne RRA, Stevens GA, White RA, Smith JL, Flaxman SR, Price H, et al. Causes of vision loss worldwide, 1990-2010: a systematic analysis. *Lancet Glob Health*. 2013;1:e339–49. [https://doi.org/10.1016/S2214-109X\(13\)70113-X](https://doi.org/10.1016/S2214-109X(13)70113-X).
2. Holden BA, Fricke TR, Wilson DA, Jong M, Naidoo KS, Sankaridurg P, et al. Global prevalence of myopia and high myopia and temporal trends from 2000 through 2050. *Ophthalmology*. 2016;123:1036–42. <https://doi.org/10.1016/j.ophtha.2016.01.006>.
3. Ding B-Y, Shih Y-F, Lin LLK, Hsiao CK, Wang I-J. Myopia among schoolchildren in East Asia and Singapore. *Surv Ophthalmol*. 2017;62:677–97. <https://doi.org/10.1016/j.survophthal.2017.03.006>.
4. Tsai T-H, Liu Y-L, Ma I-H, Su C-C, Lin C-W, Lin LL-K, et al. Evolution of the prevalence of myopia among Taiwanese schoolchildren: a review of survey data from 1983 through 2017. *Ophthalmology*. 2021;128:290–301. <https://doi.org/10.1016/j.ophtha.2020.07.017>.
5. Morgan IG, Ohno-Matsui K, Saw S-M. Myopia. *Lancet*. 2012;379:1739–48. [https://doi.org/10.1016/S0140-6736\(12\)60272-4](https://doi.org/10.1016/S0140-6736(12)60272-4).
6. Bullimore MA, Ritchey ER, Shah S, Leveziel N, Bourne RRA, Flitcroft DI. The risks and benefits of myopia control. *Ophthalmology*. 2021;128:1561–79. <https://doi.org/10.1016/j.ophtha.2021.04.032>.
7. Han X, Ong J-S, An J, Craig JE, Gharahkhani P, Hewitt AW, et al. Association of myopia and intraocular pressure with retinal detachment in European descent participants of the UK Biobank Cohort: a Mendelian randomization study. *JAMA Ophthalmol*. 2020;138:671–8. <https://doi.org/10.1001/jamaophthalmol.2020.1231>.
8. Mitry D, Charteris DG, Fleck BW, Campbell H, Singh J. The epidemiology of rhegmatogenous retinal detachment: geographical variation and clinical associations. *Br J Ophthalmol*. 2010;94:678–84. <https://doi.org/10.1136/bjo.2009.157727>.
9. Achour H, Thomseth VM, Kvaløy JT, Krohn J, Utheim TP, Forsaa VA. Substantial increase in the incidence of rhegmatogenous retinal detachment in Western Norway over 20 years. *Acta Ophthalmol*. 2022;100(7):763–8. <https://doi.org/10.1111/aos.15119>.
10. Sodhi A, Leung L-S, Do DV, Gower EW, Schein OD, Handa JT. Recent trends in the management of rhegmatogenous retinal detachment. *Surv Ophthalmol*. 2008;53:50–67. <https://doi.org/10.1016/j.survophthal.2007.10.007>.
11. Golubnitschaja O, Costigliola V, EPMA. General report & recommendations in predictive, preventive and personalised medicine 2012: white paper of the European Association for Predictive, Preventive and Personalised Medicine. *EPMA J*. 2012;3:14. <https://doi.org/10.1186/1878-5085-3-14>.
12. Golubnitschaja O, Potuznik P, Polivka J, Pesta M, Kaverina O, Pieper CC, et al. Ischemic stroke of unclear aetiology: a case-by-case analysis and call for a multi-professional predictive, preventive and personalised approach. *EPMA J*. 2022;13:535–45. <https://doi.org/10.1007/s13167-022-00307-z>.
13. Lin H-J, Wei C-C, Chang C-Y, Chen T-H, Hsu Y-A, Hsieh Y-C, et al. Role of Chronic inflammation in myopia progression: clinical evidence and experimental validation. *EBioMedicine*. 2016;10:269–81. <https://doi.org/10.1016/j.ebiom.2016.07.021>.
14. Wojciechowski R, Yee SS, Simpson CL, Bailey-Wilson JE, Stambolian D. Matrix metalloproteinases and educational attainment in refractive error: evidence of gene-environment interactions in the Age-Related Eye Disease Study. *Ophthalmology*. 2013;120:298–305. <https://doi.org/10.1016/j.ophtha.2012.07.078>.
15. Augustine J, Pavlou S, Ali I, Harkin K, Ozaki E, Campbell M, et al. IL-33 deficiency causes persistent inflammation and severe


- neurodegeneration in retinal detachment. *J Neuroinflammation*. 2019;16:251. <https://doi.org/10.1186/s12974-019-1625-y>.
16. Dai Y, Wu Z, Sheng H, Zhang Z, Yu M, Zhang Q. Identification of inflammatory mediators in patients with rhegmatogenous retinal detachment associated with choroidal detachment. *Mol Vis*. 2015;21:417–27.
  17. Bertele N, Karabatsiakos A, Buss C, Talmon A. How biomarker patterns can be utilized to identify individuals with a high disease burden: a bioinformatics approach towards predictive, preventive, and personalized (3P) medicine. *EPMA J*. 2021;12:507–16. <https://doi.org/10.1007/s13167-021-00255-0>.
  18. Phene S, Dunn RC, Hammel N, Liu Y, Krause J, Kitade N, et al. Deep learning and glaucoma specialists: the relative importance of optic disc features to predict glaucoma referral in fundus photographs. *Ophthalmology*. 2019;126:1627–39. <https://doi.org/10.1016/j.ophtha.2019.07.024>.
  19. Li F, Su Y, Lin F, Li Z, Song Y, Nie S, et al. A deep-learning system predicts glaucoma incidence and progression using retinal photographs. *J Clin Invest*. 2022;132:e157968. <https://doi.org/10.1172/JCI157968>.
  20. Baek SU, Lee WJ, Park KH, Choi HJ. Health screening program revealed risk factors associated with development and progression of papillomacular bundle defect. *EPMA J*. 2021;12:41–55. <https://doi.org/10.1007/s13167-021-00235-4>.
  21. Quek TC, Takahashi K, Kang HG, Thakur S, Deshmukh M, Tseng RMWW, et al. Predictive, preventive, and personalized management of retinal fluid via computer-aided detection app for optical coherence tomography scans. *EPMA J*. 2022;13:547–60. <https://doi.org/10.1007/s13167-022-00301-5>.
  22. Golubnitschaja O, Baban B, Boniolo G, Wang W, Bubnov R, Kapalla M, et al. Medicine in the early twenty-first century: paradigm and anticipation - EPMA position paper 2016. *EPMA J*. 2016;7:23. <https://doi.org/10.1186/s13167-016-0072-4>.
  23. Shen Y, Wang L, Jian W, Shang J, Wang X, Ju L, et al. Big-data and artificial-intelligence-assisted vault prediction and EVO-ICL size selection for myopia correction. *Br J Ophthalmol*. 2023;107(2):201–6. <https://doi.org/10.1136/bjophthalmol-2021-319618>.
  24. Li S, Shao M, Li Y, Li X, Wan Y, Sun X, et al. Relationship between oxidative stress biomarkers and visual field progression in patients with primary angle closure glaucoma. *Oxid Med Cell Longev*. 2020;2020:2701539. <https://doi.org/10.1155/2020/2701539>.
  25. Li S, Shao M, Li D, Tang B, Cao W, Sun X. Association of serum uric acid levels with primary open-angle glaucoma: a 5-year case-control study. *Acta Ophthalmol*. 2019;97:e356–63. <https://doi.org/10.1111/aos.13789>.
  26. Li S, Zhang H, Shao M, Li Y, Song Y, Sun X, et al. Association between 17- $\beta$ -estradiol and interleukin-8 and visual field progression in postmenopausal women with primary angle closure glaucoma. *Am J Ophthalmol*. 2020;217:55–67. <https://doi.org/10.1016/j.ajo.2020.04.033>.
  27. Li S, Qiu Y, Yu J, Shao M, Li Y, Cao W, et al. Association of systemic inflammation indices with visual field loss progression in patients with primary angle-closure glaucoma: potential biomarkers for 3P medical approaches. *EPMA J*. 2021;12:659–75. <https://doi.org/10.1007/s13167-021-00260-3>.
  28. Li S, Shao M, Wan Y, Tang B, Sun X, Cao W. Relationship between ocular biometry and severity of primary angle-closure glaucoma: relevance for predictive, preventive, and personalized medicine. *EPMA J*. 2019;10:261–71. <https://doi.org/10.1007/s13167-019-00174-1>.
  29. Zhang A, Ning L, Han J, Ma Y, Ma Y, Cao W, et al. Neutrophil-to-lymphocyte ratio as a potential biomarker of neovascular glaucoma. *Ocul Immunol Inflamm*. 2021;29:417–24. <https://doi.org/10.1080/09273948.2019>.
  30. Song W, Qin Z, Hu X, Han H, Li A, Zhou X, et al. Using Bayesian networks with Tabu-search algorithm to explore risk factors for hyperhomocysteinemia. *Sci Rep*. 2023;13:1610. <https://doi.org/10.1038/s41598-023-28123-z>.
  31. Yang Y, Huo H, Jiang J, Sun X, Guan Y, Guo X, et al. Clinical decision-making framework against over-testing based on modeling implicit evaluation criteria. *J Biomed Inform*. 2021;119:103823. <https://doi.org/10.1016/j.jbi.2021.103823>.
  32. Obuchowski NA, Zhou X-H. Prospective studies of diagnostic test accuracy when disease prevalence is low. *Biostatistics*. 2002;3:477–92. <https://doi.org/10.1093/biostatistics/3.4.477>.
  33. Li J, Fine J. On sample size for sensitivity and specificity in prospective diagnostic accuracy studies. *Stat Med*. 2004;23:2537–50. <https://doi.org/10.1002/sim.1836>.
  34. Robba C, Cardim D, Tajsic T, Pietersen J, Bulman M, Donnelly J, et al. Ultrasound non-invasive measurement of intracranial pressure in neurointensive care: a prospective observational study. *PLoS Med*. 2017;14:e1002356. <https://doi.org/10.1371/journal.pmed.1002356>.
  35. Xing R, Niu S, Gao X, Liu T, Fan W, Chen Y. Weakly supervised serous retinal detachment segmentation in SD-OCT images by two-stage learning. *Biomed Opt Express*. 2021;12:2312–27. <https://doi.org/10.1364/BOE.416167>.
  36. Ohsugi H, Tabuchi H, Enno H, Ishitobi N. Accuracy of deep learning, a machine-learning technology, using ultra-wide-field fundus ophthalmoscopy for detecting rhegmatogenous retinal detachment. *Sci Rep*. 2017;7:9425. <https://doi.org/10.1038/s41598-017-09891-x>.
  37. Li Z, Guo C, Nie D, Lin D, Zhu Y, Chen C, et al. Deep learning for detecting retinal detachment and discerning macular status using ultra-widefield fundus images. *Commun Biol*. 2020;3:15. <https://doi.org/10.1038/s42003-019-0730-x>.
  38. Li J, Wang L, Gao Y, Liang Q, Chen L, Sun X, et al. Automated detection of myopic maculopathy from color fundus photographs using deep convolutional neural networks. *Eye Vis (Lond)*. 2022;9:13. <https://doi.org/10.1186/s40662-022-00285-3>.
  39. Li Y, Feng W, Zhao X, Liu B, Zhang Y, Chi W, et al. Development and validation of a deep learning system to screen vision-threatening conditions in high myopia using optical coherence tomography images. *Br J Ophthalmol*. 2022;106:633–9. <https://doi.org/10.1136/bjophthalmol-2020-317825>.
  40. Eijk ESV, Busschbach JJV, Timman R, Monteban HC, Vissers JMH, van Meurs JC. What made you wait so long? Delays in presentation of retinal detachment: knowledge is related to an attached macula. *Acta Ophthalmol*. 2016;94:434–40. <https://doi.org/10.1111/aos.13016>.
  41. Wu J, Zan X, Gao L, Zhao J, Fan J, Shi H, et al. A machine learning method for identifying lung cancer based on routine blood indices: qualitative feasibility study. *JMIR Med Inform*. 2019;7:e13476. <https://doi.org/10.2196/13476>.
  42. Podnar S, Kukar M, Gunčar G, Notar M, Gošnjak N, Notar M. Diagnosing brain tumours by routine blood tests using machine learning. *Sci Rep*. 2019;9:14481. <https://doi.org/10.1038/s41598-019-51147-3>.
  43. Zhan J, Chen W, Cheng L, Wang Q, Han F, Cui Y. Diagnosis of asthma based on routine blood biomarkers using machine learning. *Comput Intell Neurosci*. 2020;2020:8841002. <https://doi.org/10.1155/2020/8841002>.
  44. Plante TB, Blau AM, Berg AN, Weinberg AS, Jun IC, Tapson VF, et al. Development and external validation of a machine learning tool to rule out COVID-19 among adults in the emergency department using routine blood tests: a large, multicenter, real-world study. *J Med Internet Res*. 2020;22:e24048. <https://doi.org/10.2196/24048>.
  45. Tanriver G, Kocagoncu E. Additive pre-diagnostic and diagnostic value of routine blood-based biomarkers in the

- detection of colorectal cancer in the UK Biobank cohort. *Sci Rep.* 2023;13:1367. <https://doi.org/10.1038/s41598-023-28631-y>.
46. Araújo DC, Veloso AA, Borges KBG, Carvalho M, das G. Prognosing the risk of COVID-19 death through a machine learning-based routine blood panel: a retrospective study in Brazil. *Int J Med Inform.* 2022;165:104835. <https://doi.org/10.1016/j.ijmedinf.2022.104835>.
  47. Nicholson BD, Aveyard P, Koshiaris C, Perera R, Hamilton W, Oke J, et al. Combining simple blood tests to identify primary care patients with unexpected weight loss for cancer investigation: clinical risk score development, internal validation, and net benefit analysis. *PLoS Med.* 2021;18:e1003728. <https://doi.org/10.1371/journal.pmed.1003728>.
  48. Alibet Y, Levytska G, Umanets N, Pasychnikova N, Henrich PB. Ciliary body thickness changes after preoperative anti-inflammatory treatment in rhegmatogenous retinal detachment complicated by choroidal detachment. *Graefes Arch Clin Exp Ophthalmol.* 2017;255:1503–8. <https://doi.org/10.1007/s00417-017-3673-2>.
  49. Wei Y, Wang N, Chen F, Wang H, Bi C, Zu Z, et al. Vitrectomy combined with periocular/intravitreal injection of steroids for rhegmatogenous retinal detachment associated with choroidal detachment. *Retina.* 2014;34:136–41. <https://doi.org/10.1097/IAE.0b013e3182923463>.
  50. Sharma T, Gopal L, Reddy RK, Kasinathan N, Shah NA, Sulochana KN, et al. Primary vitrectomy for combined rhegmatogenous retinal detachment and choroidal detachment with or without oral corticosteroids: a pilot study. *Retina.* 2005;25:152–7. <https://doi.org/10.1097/00006982-200502000-00006>.
  51. Jia Y-P, Sun L, Yu H-S, Liang L-P, Li W, Ding H, et al. The pharmacological effects of lutein and zeaxanthin on visual disorders and cognition diseases. *Molecules.* 2017;22:610. <https://doi.org/10.3390/molecules22040610>.
  52. Daruich A, Jaworski T, Henry H, Zola M, Youale J, Parenti L, et al. Oral ursodeoxycholic acid crosses the blood retinal barrier in patients with retinal detachment and protects against retinal degeneration in an ex vivo model. *Neurotherapeutics.* 2021;18:1325–38. <https://doi.org/10.1007/s13311-021-01009-6>.
  53. Golubnitschaja O, Topolcan O, Kucera R, Costigliola V, EPMA. 10th Anniversary of the European Association for Predictive, Preventive and Personalised (3P) Medicine - EPMA World Congress Supplement 2020. *EPMA J.* 2020;11:1–133. <https://doi.org/10.1007/s13167-020-00206-1>.

**Publisher's note** Springer Nature remains neutral with regard to jurisdictional claims in published maps and institutional affiliations.

Springer Nature or its licensor (e.g. a society or other partner) holds exclusive rights to this article under a publishing agreement with the author(s) or other rightsholder(s); author self-archiving of the accepted manuscript version of this article is solely governed by the terms of such publishing agreement and applicable law.

## Authors and Affiliations

Shengjie Li<sup>1,2,3,4</sup>  · Meiyang Li<sup>2,3,4,5,6</sup> · Jianing Wu<sup>1</sup> · Yingzhu Li<sup>1</sup> · Jianping Han<sup>1</sup> · Wenjun Cao<sup>1,2,3,4</sup> · Xingtao Zhou<sup>2,3,4,5,6</sup>

✉ Wenjun Cao  
wgkjk@aliyun.com

✉ Xingtao Zhou  
doctzhouxingtao@163.com

<sup>1</sup> Department of Clinical Laboratory, Eye & ENT Hospital, Shanghai Medical College, Fudan University, Shanghai, China

<sup>2</sup> Eye Institute and Department of Ophthalmology, Eye & ENT Hospital of Fudan University, Shanghai, China

<sup>3</sup> NHC Key Laboratory of Myopia, Shanghai, China

<sup>4</sup> Shanghai Research Center of Ophthalmology and Optometry, Shanghai, China

<sup>5</sup> Key Laboratory of Myopia, Chinese Academy of Medical Sciences, Shanghai, China

<sup>6</sup> Shanghai Engineering Research Center of Laser and Autostereoscopic 3D for Vision Care, Shanghai, China